

Degenerate parametric amplifiers with a squeezed pump

Netta Cohen

Department of Physics, Technion-Israel Institute of Technology, Haifa 32000, Israel

Samuel L. Braunstein

Department of Chemical Physics, The Weizmann Institute of Science, Rehovot 76100, Israel

(Received 14 December 1994)

We study the effects of squeezed pump fluctuations in the degenerate parametric amplifier on signal squeezing. We find, both through semiclassical calculations and through several detailed analytic methods, that pump squeezing is responsible for two competing processes: Reduced pump phase fluctuations improve limitations to squeezing; at the same time, increased pump intensity fluctuations can lead to a “spillover” of pump fluctuations onto negative pump phases and a consequent reduction in signal squeezing.

PACS number(s): 42.50.Dv, 42.50.Lc, 42.65.-k, 03.65.Bz

I. INTRODUCTION

The degenerate parametric amplifier (DPA) is a nonlinear device: It converts pump photons of frequency ω_p to pairs of correlated signal photons centered around frequency $\omega = \omega_p/2$ [1]. The Hamiltonian that governs the behavior of this system in the Schrödinger picture is

$$\begin{aligned} \hat{\mathcal{H}}(t) &= \hat{\mathcal{H}}_0 + \hat{\mathcal{H}}_{\text{int}} \\ &= \hbar\omega_s \hat{a}^{(S)\dagger} \hat{a}^{(S)} + \hbar\omega_p \hat{a}_p^{(S)\dagger} \hat{a}_p^{(S)} \\ &\quad + \frac{i\hbar\kappa}{2} \left(\hat{a}^{(S)\dagger 2} \hat{a}_p^{(S)} - \hat{a}^{(S)2} \hat{a}_p^{(S)\dagger} \right), \end{aligned} \quad (1.1)$$

where $\hat{a}_p^{(S)}$ and $\hat{a}^{(S)}$ are the pump and signal annihilation operators and κ is the coupling constant between the signal field and the pump field. This coupling constant is proportional to the second-order susceptibility of the nonlinear medium $\chi^{(2)}$ [2].

One interesting and useful property of the DPA is its ability to generate a squeezed signal [3–5]. In this paper, we are interested in the limitations to signal squeezing due to the pump’s quantum mechanical fluctuations. We develop analytic methods for calculating the long-time evolution of nonlinear devices and apply these tools to the degenerate parametric amplifier. The analytic results that we obtain are (essentially) independent of the initial signal and pump states. Thus the evolution of the system for various initial states can be obtained directly. In particular, we present the results for an initially squeezed-coherent pump and a signal initially in vacuum. We also compare our results for a pump with zero initial squeezing (i.e., a coherent pump) with other works.

The evolution of the DPA and the limits to squeezing have been studied by various methods, for the special case of an initially coherent pump and a signal in vacuum. Hillery and Zubairy [6] were the first to obtain the semiclassical corrections [that is, corrections to $O(1/\bar{N})$, where \bar{N} denotes the mean number of pump photons] using a path integral technique. These semiclassical corrections were confirmed by Crouch and Braunstein (CB)

[7], who tackled the problem from several directions. One approach was to use the positive- P representation to derive Fokker-Planck equations that were then used to obtain stochastic differential equations; iterating these equations yielded the semiclassical solution. In addition, CB calculated the explicit corrections for squeezing to $O(1/\bar{N}^2)$ in two ways: through an analytic calculation, based on perturbation theoretic techniques, and using a seminumerical technique. Kinsler, Fernée, and Drummond (KFD) [8] took a numerical approach. They computed solutions in the several ways. Their most successful long-time solution for the squeezing in the DPA was obtained through a computer simulation of the stochastic differential equations of CB. In contrast, our paper is based, to a large extent, on the analytic techniques developed by CB.

Recently, Hillery, Yu, and Bergou [9] studied the signal evolution in the DPA in the case of an initially squeezed pump and solved it in the limit of a weak pump (using semiclassical methods). These results were confirmed and extended by Bužek and Drobný [10,11]. In what follows, we present two methods for approaching this problem and the results obtained for coherent and squeezed pumps (with the signal initially in vacuum) for weak as well as intense pumps. Both of these methods employ perturbation theoretic techniques. Thus finite-order perturbation theory will serve as the starting point of this work. One way of improving these truncated results is by applying the method of Padé approximants. In the second method, dominant terms are selected and summed to all orders of the expansion parameter ($1/\alpha$, where α is the pump amplitude). Both methods yield analytic expressions for the time-evolved operators. The dynamics of the system is studied by calculating all quadratic matrix elements of the signal and pump quadrature operators (i.e., quadrature variances, correlations, and commutators). In addition, we used these matrix elements in a “commutator test,” which is applied to determine the range of validity of our results. We find that the long-time behavior of the system is described as accurately by

our analytic approaches as the best numerical methods available to date [8]. Moreover, our treatment helps provide an intuitive understanding of previously obtained results for a DPA with a weak, squeezed pump [6,10,11].

In Sec. II we review the semiclassical approach to the DPA. We show how the effect of pump phase and amplitude fluctuations on the signal evolution may be taken into consideration within this model, for the cases of coherent and squeezed-coherent pumps. In Secs. III and IV we present the two analytic methods we have developed. The commutator test and other suggested tests are discussed in Sec. V. Finally, our results, along with a comparison with results in the literature, are given in Secs. VI and VII for coherent and squeezed pumps, respectively.

II. SEMICLASSICAL APPROACH

We begin by examining the signal evolution in the DPA in the presence of a very strong pump, using the semiclassical approach. This method assumes a “classical” (constant) pump with some fixed fluctuations and a quantum mechanical signal. We start by applying the parametric approximation (constant pump with no fluctuations) to the interaction picture Hamiltonian and deriving equations of motion for the signal quadrature operators thereof. This may be regarded as a zeroth-order solution to the problem. The first-order solution would then include the pump fluctuations and hence their effect on the signal. Higher-order solutions must take into account the pump’s evolution as well; this extends beyond the scope of the semiclassical approach and will be discussed in Secs. III and IV. Thus the semiclassical calculation consists of first finding the signal quadrature variances under the parametric approximation and then including the pump fluctuations phenomenologically. (These fluctuations are ultimately due to the pump’s quantum mechanical nature.) We consider both phase and intensity fluctuations of the pump and calculate the optimal squeezing of the signal and the corresponding interaction time for the case of a coherent-state pump. We then extend our results and apply them to the case of a squeezed-pump DPA.

We would like to remove the fast (optical) rotation of the pump and signal fields and therefore move from the Schrödinger picture of Eq. (1.1) to the interaction picture:

$$\hat{\mathcal{H}}_{\text{int}}^{(I)} = \frac{i\hbar\kappa}{2} (\hat{a}^{\dagger 2} \hat{a}_p - \hat{a}^2 \hat{a}_p^\dagger) \quad (2.1)$$

(up to an arbitrary phase that has been absorbed in the field operators). We shall work in the interaction picture henceforth.

In the limit of a strong pump, its uncertainty has a negligible effect on the signal. Under these circumstances, the pump behaves classically, thus justifying the parametric approximation, in which the pump operator is replaced by a c number:

$$\hat{a}_p \rightarrow \alpha e^{i\phi}, \quad (2.2)$$

where α is real. In fact, the classical pump approximation requires an additional, more subtle assumption, namely, that the nonlinear susceptibility of the medium $\chi^{(2)}$ (or the coupling constant κ) be small. This ensures that the nonlinear gain coefficient in the medium is small as well [12]. Gain implies that the signal is amplified at the expense of pump depletion—a quantum mechanical effect that violates the semiclassical (SC) constant pump assumption. The constant pump requirement also places a time restriction on the validity of the parametric approximation, for no matter how small the nonlinear gain coefficient, the gain will inevitably become significant after some interaction time.

The single-mode interaction Hamiltonian, rewritten with classical pump variables, is

$$\hat{\mathcal{H}}_{\text{int}}^{\text{SC}} = \frac{i\hbar\kappa\alpha}{2} [\hat{a}^{\dagger 2}(t) e^{i\phi} - \hat{a}^2(t) e^{-i\phi}], \quad (2.3)$$

and the Heisenberg equations of motion are

$$\frac{d\hat{a}(t)}{dt} = \frac{i}{\hbar} [\hat{\mathcal{H}}_{\text{int}}^{\text{SC}}, \hat{a}(t)] = \kappa\alpha e^{i\phi} \hat{a}^\dagger(t), \quad (2.4a)$$

$$\frac{d\hat{a}^\dagger(t)}{dt} = \frac{i}{\hbar} [\hat{\mathcal{H}}_{\text{int}}^{\text{SC}}, \hat{a}^\dagger(t)] = \kappa\alpha e^{-i\phi} \hat{a}(t). \quad (2.4b)$$

[The evolution operator for this Hamiltonian,

$$\hat{U} = \exp\left(-\frac{i}{\hbar} \hat{\mathcal{H}}_{\text{int}}^{(I)} t\right) = \exp\left[\frac{\kappa\alpha t}{2} (\hat{a}^{\dagger 2} e^{i\phi} - \hat{a}^2 e^{-i\phi})\right], \quad (2.5)$$

is none other than the squeezing operator $\hat{S} = \hat{S}(\kappa\alpha t, \phi)$, making the DPA the prototypic squeezing device.]

By assuming a classical pump that squeezes (or amplifies) the signal exactly along the $\phi/2 + \pi/2$ (or $\phi/2$) direction, we have removed any mixing or coupling in the signal behavior along these two quadrature axes (aligned with $\phi/2 + \pi/2$ and $\phi/2$). It is therefore natural to define a set of two signal quadrature operators that decouple Eqs. (2.4):

$$\hat{X}_1(t) = \frac{1}{2} [\hat{a}(t) e^{-i\phi/2} + \hat{a}^\dagger(t) e^{i\phi/2}], \quad (2.6a)$$

$$\hat{X}_2(t) = -\frac{i}{2} [\hat{a}(t) e^{-i\phi/2} - \hat{a}^\dagger(t) e^{i\phi/2}]. \quad (2.6b)$$

We note that the signal phase $\phi/2$ accumulates at half the rate of the pump phase ϕ .

Let u , a dimensionless evolution parameter hereafter referred to simply as time, be defined by

$$u = \kappa\alpha t. \quad (2.7)$$

The equations of motion in terms of these new variables are trivial to solve:

$$\frac{d\hat{X}_1(u)}{du} = \hat{X}_1(u) \Rightarrow \hat{X}_1(u) = \hat{X}_1(0) e^u, \quad (2.8a)$$

$$\frac{d\hat{X}_2(u)}{du} = -\hat{X}_2(u) \Rightarrow \hat{X}_2(u) = \hat{X}_2(0) e^{-u}. \quad (2.8b)$$

For a signal initially in the vacuum state,

$$\langle \Delta \hat{X}_1^{(0)2} \rangle \equiv \langle \Delta \hat{X}_1^2(u) \rangle = \frac{1}{4} e^{2u}, \quad (2.9a)$$

$$\langle \Delta \hat{X}_2^{(0)2} \rangle \equiv \langle \Delta \hat{X}_2^2(u) \rangle = \frac{1}{4} e^{-2u}. \quad (2.9b)$$

The squeezing (amplification) along the \hat{X}_2 (\hat{X}_1) quadrature is unlimited in this approximation. This is the zeroth-order solution (see Fig. 1).

The next step in the calculation—the first-order solution—takes into account the quantum nature of the pump, i.e., its phase and intensity fluctuations. We begin by including the phase noise $\Delta\phi$. For a real, coherent pump state $|\alpha = \sqrt{N}\rangle$, the uncertainty in the phase is given by

$$\langle \Delta\phi^2 \rangle = \langle \phi^2 \rangle = \frac{1}{4N} + O\left(\frac{1}{N^2}\right) \quad (2.10)$$

(see Fig. 2). The effect of these fluctuations on the quadrature operators is to squeeze the signal along slightly rotated quadratures:

$$\hat{X}_1^{(1)} = \hat{X}_1 \cos(\Delta\phi/2) + \hat{X}_2 \sin(\Delta\phi/2), \quad (2.11)$$

$$\hat{X}_2^{(1)} = \hat{X}_2 \cos(\Delta\phi/2) - \hat{X}_1 \sin(\Delta\phi/2), \quad (2.12)$$

where $\langle (\Delta \hat{X}_i^{(1)})^2 \rangle$ are the first-order correction terms to the parametric approximation. Adding these to the previous results [Eqs. (2.9b)]

$$\langle \Delta \hat{X}_2^2(u) \rangle = \langle (\Delta \hat{X}_2^{(0)})^2 \rangle + \frac{1}{4} \langle (\Delta \hat{X}_2^{(1)})^2 \rangle, \quad (2.13)$$

we obtain our first semiclassical result

$$\begin{aligned} \langle \Delta \hat{X}_2^2(u) \rangle &\simeq \frac{1}{4} e^{-2u} + \frac{1}{16} e^{2u} \langle \phi^2 \rangle \\ &\quad + \frac{1}{4} e^{-2u} \left(1 - \frac{1}{4} \langle \phi^2 \rangle \right) \\ &\simeq \frac{1}{4} e^{-2u} + \frac{1}{64N} (e^{2u} - e^{-2u}). \end{aligned} \quad (2.14)$$

Typically, we are interested in studying pumps with $\bar{N} \gg$

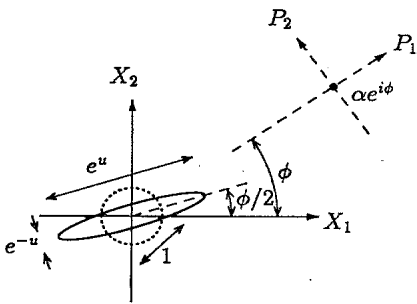


FIG. 1. Classical pump DPA: A classical pump with a coherent amplitude $\alpha e^{i\phi}$ is drawn as a black dot. The pump quadrature axes are aligned with the pump phase. The dotted circle represents the signal's initial vacuum state with $\Delta \hat{X}_1 = \Delta \hat{X}_2 = 1/2$. The time-evolved signal is drawn as a solid ellipse, aligned with the signal phase $\phi/2$. In this ideal model, $\Delta \hat{X}_1(u) = e^u$ and $\Delta \hat{X}_2(u) = e^{-u}$.

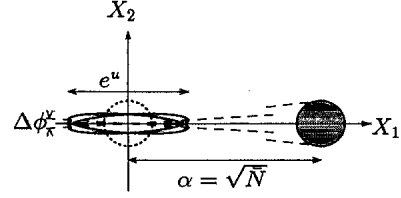


FIG. 2. Coherent pump DPA: A real, coherent pump (with $\langle \phi \rangle = 0$), drawn in gray, now squeezes the signal along slightly rotated quadratures. The dotted circle and the solid ellipses represent the initial vacuum state and the time-evolved squeezed-vacuum states of the signal, respectively. The first-order effect of the pump phase fluctuations is to impose limits on the amount of signal squeezing achievable [$\tan(\Delta\phi/2) \simeq \Delta P_2/\bar{N}$].

1 for times $u \gtrsim 1$; in that case, the last term in the equation may be dropped, and we obtain [13]

$$\langle \Delta \hat{X}_2^2(u) \rangle \simeq \frac{1}{4} e^{-2u} + \frac{1}{64N} e^{2u}. \quad (2.15)$$

Hence the \hat{X}_2 variance is limited with a minimum of

$$\langle \Delta \hat{X}_2^2(u) \rangle_{\min} \simeq \frac{1}{8\sqrt{N}} \left(1 + \frac{1}{4N} \right) \simeq \frac{1}{8\sqrt{N}} \quad (2.16)$$

at a time

$$u_{\min} \simeq \frac{1}{4} \ln(16\bar{N} + 1) \simeq \frac{1}{4} \ln(16\bar{N}). \quad (2.17)$$

Recall that u is a scaled time parameter that depends on the intensity of the pump. Thus, for a given length of interaction traversed z , the optimal time t_{\min} can dictate the intensity of the pump:

$$t_{\min} = \frac{n_0 z}{c} \simeq \frac{1}{4\kappa\sqrt{N}} \ln(16\bar{N} + 1). \quad (2.18)$$

Note that the parametric approximation (classical noiseless pump) is valid only for sufficiently large \bar{N} and small dimensionless time, or when the correction term is small:

$$\frac{1}{4} e^{-2u} \gg \frac{1}{64N} (e^{2u} - e^{-2u}), \quad (2.19)$$

that is to say, before optimal squeezing is obtained.

We can further improve Eq. (2.14) by accounting for not only the phase fluctuations, but the intensity fluctuations of the pump as well. For a coherent pump,

$$\langle \Delta \bar{N} \rangle = 0, \quad (2.20a)$$

$$\langle \Delta \bar{N}^2 \rangle = \bar{N}, \quad (2.20b)$$

$$\langle \Delta \bar{N} \Delta \phi \rangle \simeq 0. \quad (2.20c)$$

Thus an expansion of the results to $O(1/\bar{N})$ gives

$$\begin{aligned} \langle \Delta \hat{X}_2^2(u) \rangle &\simeq \frac{1}{4} e^{-2u} + \frac{1}{N} \left[\frac{1}{64} (e^{2u} - e^{-2u}) \right. \\ &\quad \left. + \frac{1}{16} u e^{-2u} + \frac{1}{8} u^2 e^{-2u} \right]. \end{aligned} \quad (2.21)$$

Until now, we have assumed the pump was coherent. Consider now a squeezed pump, with a real squeezing parameter r along the \hat{P}_2 quadrature. This pump will also squeeze the signal along the \hat{X}_2 quadrature, provided its mean phase is zero. However, since the pump's phase fluctuations are reduced, the resulting limits to squeezing are not as tight.

The pump's phase uncertainty causes fluctuations in the signal that are given by

$$\langle \Delta \phi^2 \rangle = \langle \phi^2 \rangle = \frac{e^{-2r}}{4\alpha^2} + O\left(\frac{1}{\alpha^4}\right), \quad (2.22)$$

where now

$$\bar{N} = \alpha^2 + \sinh^2(r). \quad (2.23)$$

Hence the first-order correction term to the \hat{X}_2 variance becomes

$$\langle [\Delta \hat{X}_2^{(1)}(u)]^2 \rangle \simeq \frac{e^{-2r}}{64\alpha^2} (e^{2u} - e^{-2u}) \simeq \frac{e^{-2r}}{64\alpha^2} e^{2u}, \quad (2.24)$$

where the last approximation is valid for sufficiently long times. Including number fluctuations as well yields the variance to $O(1/\alpha^2)$:

$$\begin{aligned} \langle \Delta \hat{X}_2^2(u) \rangle \simeq & \frac{1}{4} e^{-2u} + \frac{1}{\alpha^2} \left[\frac{e^{-2r}}{64} (e^{2u} - e^{-2u}) \right. \\ & \left. + \frac{e^{2r}}{16} u e^{-2u} + \frac{e^{2r}}{8} u^2 e^{-2u} \right]. \end{aligned} \quad (2.25)$$

Here we used $\langle \Delta \bar{N}^2 \rangle \simeq \alpha^2 e^{2r}$. As u gets larger ($u \gtrsim 1$), only the first (growing) term in Eq. (2.24) remains significant and the minimum variance becomes

$$\langle \Delta \hat{X}_2^2(u) \rangle_{\min} \simeq \frac{e^{-2r}}{8\alpha} \quad \text{at} \quad u_{\min} \simeq \frac{1}{2} [r + \ln(4\alpha)]. \quad (2.26)$$

The above semiclassical calculation regarding the limitations to squeezing in a DPA with a squeezed pump predicts that (for a pump with a fixed coherent amplitude) as the squeezing parameter of the pump increases, the minimum variance of the squeezed quadrature declines exponentially whereas the time at which the minimum is attained grows linearly. However, before the minimum u_{\min} is reached, the signal squeezing is independent of r . We expect this to be an accurate statement because it concerns a time interval over which the semiclassical assumptions are still valid (see also [6,7,9]). This conclusion does not apply in the case of an exceedingly weak pump. In that case, we are interested in knowing how the signal evolves at very short times and return to the full semiclassical result [Eq. (2.25)]. We find that the terms that decay in time have an e^{2r} dependence that results in increased noise in the signal. Therefore, for sufficiently weak pumps, pump squeezing may cause more harm than good [9].

III. DOMINANT TERM ITERATION AND SUMMATION PROCEDURE

The Heisenberg equations of motion for the single-mode parametric amplifier [from Eq. (2.1)] are

$$\frac{d\hat{a}}{dt} = \kappa \hat{a}_p \hat{a}^\dagger, \quad (3.1a)$$

$$\frac{d\hat{a}_p}{dt} = -\frac{\kappa}{2} \hat{a}^2. \quad (3.1b)$$

In order to study the time-evolved fluctuations or uncertainty in the signal and pump fields of the DPA, it is convenient to rewrite these equations of motion in terms of field-quadrature operators \hat{Q}_i , initially chosen so that

$$\hat{Q}_i(0) = \Delta \hat{Q}_i(0) \quad i = 1, 2, \quad (3.2)$$

i.e., treating effective signal and pump states centered around the origin in their respective phase spaces.

Two models are of particular interest: first, a signal initially in the vacuum state that is squeezed by a coherent pump and second, a vacuum, squeezed by a phase-squeezed pump. Let the signal quadrature operators be [14]

$$\hat{X}_1 = \frac{1}{2}(\hat{a} + \hat{a}^\dagger), \quad \hat{X}_2 = -\frac{i}{2}(\hat{a} - \hat{a}^\dagger), \quad (3.3)$$

i.e., $\hat{a} = \hat{X}_1 + i\hat{X}_2$ and the pump quadrature operators

$$\alpha + \hat{P}_1 = \frac{1}{2}(\hat{a}_p + \hat{a}_p^\dagger), \quad \hat{P}_2 = -\frac{i}{2}(\hat{a}_p - \hat{a}_p^\dagger) \quad (3.4)$$

or $\hat{a}_p = \alpha + \hat{P}_1 + i\hat{P}_2$. That is, by choosing a pump phase $\langle \phi_p \rangle = 0$, the effective displacement of the pump state is performed along the real quadrature axis \hat{P}_1 . A coherent pump will now be given by an effective vacuum, whereas a squeezed pump will be given by a squeezed vacuum state.

Using these operators, the equations of motion may be written in integral form [7]

$$\begin{aligned} \hat{X}_1(u) = & e^u \hat{X}_1(0) + \frac{e^u}{\alpha} \int_0^u du' e^{-u'} [\hat{X}_1(u') \hat{P}_1(u') \\ & + \hat{X}_2(u') \hat{P}_2(u')], \end{aligned} \quad (3.5a)$$

$$\begin{aligned} \hat{X}_2(u) = & e^{-u} \hat{X}_2(0) + \frac{e^{-u}}{\alpha} \int_0^u du' e^{u'} [\hat{X}_1(u') \hat{P}_2(u') \\ & - \hat{X}_2(u') \hat{P}_1(u')], \end{aligned} \quad (3.5b)$$

$$\hat{P}_1(u) = \hat{P}_1(0) - \frac{1}{2\alpha} \int_0^u du' [\hat{X}_1^2(u') - \hat{X}_2^2(u')], \quad (3.5c)$$

$$\begin{aligned} \hat{P}_2(u) = & \hat{P}_2(0) - \frac{1}{2\alpha} \int_0^u du' [\hat{X}_1(u') \hat{X}_2(u') \\ & + \hat{X}_2(u') \hat{X}_1(u')]. \end{aligned} \quad (3.5d)$$

These coupled time-dependent equations [Eqs. (3.5)] can be approached in various ways. One approach is to apply perturbation theoretic techniques. The equations of motion are iterated by substitution of themselves into their own integrals to successively replace terms such as $Q_i(u)$ by $Q_j(0)$. This leads to an expansion in $1/\alpha$.

The main difficulty in this method is that the number of terms grows geometrically with the order of the iteration. Hence, obtaining an answer to an accuracy of $O(1/N^2)$ requires about 1000 terms. As a result, the number of iterations performed is small. We call the result obtained from finite-order perturbation theory the truncated result.

The truncated result is especially good for large α , in which case the behavior is dominated by the terms in the lower-order iterations at least for some time. For smaller α , however, one should attempt to obtain results to all orders of $1/\alpha$. This is done by the dominant term method. To simplify the notation, let us define

$$\beta \equiv \frac{1}{\alpha} \quad (3.6)$$

One can now see that the integral equations [Eqs. (3.5)], obtained from the newly defined quadrature operators [Eqs. (3.3) and (3.4)], suggest β as an obvious choice for an expansion parameter, with each iteration adding a factor of β to the solution. For each order of β , those terms that dominate (the term "dominant" is defined below) for long times are selected and only they are used for higher-order iterations. This is justified since non-dominant terms do not contribute any dominant terms to higher orders of iterations. After a sufficient number of iterations, a pattern becomes apparent, and the dominant terms are summed to all orders of β . The dominant term approach is expected to describe the signal and pump evolution to a good accuracy both before and after optimal squeezing is achieved. An early version of the dominant term approach was first suggested by CB and used to calculate the variance of the squeezed quadrature $\langle \Delta \hat{X}_2^2 \rangle$ of a multimode parametric amplifier

to $O(1/\alpha^4)$. In this work, the method is extended to include the next-to-dominant terms in u as well and to obtain an analytic expression for these terms to all orders of β . Furthermore, the variances, correlations, and commutators of all quadrature operators are calculated. Note that the dominant term method breaks down for very small times $u \ll 1$, before the selected terms begin to dominate and for very long times $u > u_{\max}$, with u_{\max} to be determined by the commutator test.

The dominant terms in each order of β are found according to the following scheme. From Eqs. (3.5), it is clear that repeated iterations yield expressions whose time dependence is of polynomial and/or exponential form. For some quadrature operator \hat{Q} ,

$$\hat{Q} = \sum_{i=0}^{\infty} \hat{C}_i(u) \beta^i \quad (3.7)$$

The coefficients \hat{C}_i can be written in general as

$$\hat{C}_i(u) = \sum_j \hat{K}_{ij} P^{(m)}(u) e^{ju} \quad (3.8)$$

where \hat{K}_{ij} are functions of the initial quadrature operators and $P^{(m)}(u)$ is a polynomial in u of order $m \geq 0$. Denote the largest j for which $\hat{K}_{ij} \neq 0$ (for at least one i) by J . Then the dominant term of the i th order is

$$\hat{C}_{iJ}^{\text{dom}}(u) \propto \hat{K}_{iJ} u^m e^{Ju} \quad (3.9)$$

The next-to-dominant terms are calculated by the same procedure [16].

It is clear from the form of Eqs. (3.5) that discarded, less dominant terms could not contribute to dominant terms of higher order in β . For instance, for \hat{X}_1 , the first iteration gives an answer $\hat{X}_1^{(1)}(u)$ of the order of

$$\begin{aligned} \hat{X}_1^{(1)}(u) &\sim e^u \hat{X}_1(0) + \beta e^u \int_0^u du' e^{-u'} [e^{u'} \hat{X}_1(0) \hat{P}_1(0) + e^{-u'} \hat{X}_2(0) \hat{P}_2(0)] \\ &\sim e^u \hat{X}_1(0) + \beta [ue^u \hat{X}_1(0) \hat{P}_1(0) + \frac{1}{2}(1 - e^{-2u}) \hat{X}_2(0) \hat{P}_2(0)] \\ &\sim e^u \hat{X}_1(0) + \beta [ue^u \hat{X}_1(0) \hat{P}_1(0) + \frac{1}{2} \hat{X}_2(0) \hat{P}_2(0) + \dots] \end{aligned} \quad (3.10)$$

keeping dominant and next-to-dominant terms in the long-time behavior. The term proportional to e^{-2u} makes no contribution since in any future integration, the linear term will dominate. It is easy to see that this line of reasoning holds to all orders.

A close look at the dominant term solutions for the time-evolved quadrature operators up to $O(\beta^9)$ reveals that they can all be expressed in terms of converging geometric series. In general, the series representing the dominant terms have much simpler forms than those of the next-to-dominant terms. A simplified form of these solutions is given below. Note that the terms have been rearranged and grouped according to the geometric series, where the dominant terms appear in the first set of square brackets and the next-to-dominant terms follow. For the sake of clarity, the following substitutions

are introduced:

$$\begin{aligned} \hat{y} &\equiv -\frac{\beta^2 e^{2u} \hat{X}_1^2(0)}{8} \quad , \\ \hat{p}_1 &\equiv \beta u \hat{P}_1(0) \quad , \quad \hat{p}_2 \equiv \beta e^u \hat{P}_2(0) \quad . \end{aligned} \quad (3.11)$$

Also, the operators have been ordered according to the sequence $\hat{X}_1, \hat{X}_2, \hat{P}_1, \hat{P}_2$, which is obtained from the commutation relations

$$\left[\hat{X}_1, \hat{X}_2 \right] = \frac{i}{2} \quad , \quad (3.12a)$$

$$\left[\hat{P}_1, \hat{P}_2 \right] = \frac{i}{2} \quad , \quad (3.12b)$$

$$\left[\hat{X}_i, \hat{P}_j \right] = 0 \quad , \quad i, j = 1, 2 \quad . \quad (3.12c)$$

Finally, the argument ($u = 0$) is dropped:

$$\begin{aligned} \hat{X}_1^{\text{dom}(9)}(u) &= [e^u \hat{X}_1 (1 + \hat{y} + \hat{y}^2 + \hat{y}^3 + \hat{y}^4)] + e^u \hat{X}_1 (1 + 3\hat{y} + 5\hat{y}^2 + 7\hat{y}^3 + 9\hat{y}^4) \hat{p}_1 \\ &\quad + \frac{e^u}{2} \hat{X}_1 (1 + 3^2\hat{y} + 5^2\hat{y}^2 + 7^2\hat{y}^3) \hat{p}_1^2 - 2\beta e^u \hat{X}_1 (\hat{y} + 2\hat{y}^2 + 3\hat{y}^3) \hat{P}_1 \\ &\quad + \frac{i\beta^2 e^{2u}}{32} \hat{X}_1 (1 \times 3 + 2 \times 5\hat{y} + 3 \times 7\hat{y}^2 + 4 \times 9\hat{y}^3) \hat{p}_2 + (1 + 3\hat{y} + 5\hat{y}^2 + 7\hat{y}^3 + 9\hat{y}^4) \frac{\hat{X}_2 \hat{p}_2}{2}, \end{aligned} \quad (3.13a)$$

$$\begin{aligned} \hat{X}_2^{\text{dom}(9)}(u) &= \left[e^{-u} \hat{X}_2 + \hat{X}_1 (1 + \hat{y} + \hat{y}^2 + \hat{y}^3 + \hat{y}^4) \frac{\hat{p}_2}{2} \right] - e^{-u} \hat{X}_2 \hat{p}_1 + \frac{i}{8} \beta^2 u e^u \hat{X}_1 (1 + \hat{y} + \hat{y}^2 + \hat{y}^3) \\ &\quad + \hat{X}_1 (1 + 3\hat{y} + 5\hat{y}^2 + 7\hat{y}^3) \frac{\hat{p}_1 \hat{p}_2}{2} + 4u(\hat{y} + \hat{y}^2 + \hat{y}^3 + \hat{y}^4) e^{-u} \hat{X}_2 + \frac{i\beta^2 u}{8} e^u \hat{X}_1 (1 + 3\hat{y} + 5\hat{y}^2 + 7\hat{y}^3) \hat{p}_1 \\ &\quad + \frac{\hat{X}_1}{4} (1^2 + 3^2\hat{y} + 5^2\hat{y}^2 + 7^2\hat{y}^3) \hat{p}_1^2 \hat{p}_2 + 4u(\hat{y} + 3\hat{y}^2 + 5\hat{y}^3 + 7\hat{y}^4) e^{-u} \hat{X}_2 \hat{p}_1, \end{aligned} \quad (3.13b)$$

$$\begin{aligned} \hat{P}_1^{\text{dom}(9)}(u) &= \left[\hat{P}_1 + \frac{2}{\beta} (\hat{y} + \hat{y}^2 + \hat{y}^3 + \hat{y}^4 + \hat{y}^5) + \frac{4}{\beta} (\hat{y} + 2\hat{y}^2 + 3\hat{y}^3 + 4\hat{y}^4) \hat{p}_1 \right] \frac{\beta}{4} (\hat{X}_1^2 + \hat{X}_2^2) \\ &\quad + \frac{i\beta e^u}{16} (1 + 3 \times 2\hat{y} + 5 \times 3\hat{y}^2 + 7 \times 4\hat{y}^3) \hat{p}_2 - 2(\hat{y} + 3\hat{y}^2 + 5\hat{y}^3 + 7\hat{y}^4) \hat{P}_1 \\ &\quad - \frac{\beta}{4} e^u \hat{X}_1 (1 + 2\hat{y} + 3\hat{y}^2 + 4\hat{y}^3) \hat{X}_2 \hat{p}_2 + \frac{4}{\beta} (\hat{y} + 2^2\hat{y}^2 + 3^2\hat{y}^3 + 4^2\hat{y}^4) \hat{p}_1^2, \end{aligned} \quad (3.13c)$$

$$\begin{aligned} \hat{P}_2^{\text{dom}(9)}(u) &= \left[\hat{P}_2 + \frac{i\beta u}{4} - \beta u \hat{X}_1 \hat{X}_2 + 2(\hat{y} + \hat{y}^2 + \hat{y}^3 + \hat{y}^4) \hat{P}_2 \right] - \frac{\beta^2 u}{2} \hat{X}_2^2 \hat{P}_2 + \frac{i\beta u}{2} (\hat{y} + \hat{y}^2 + \hat{y}^3 + \hat{y}^4) \\ &\quad + 4(\hat{y} + 2\hat{y}^2 + 3\hat{y}^3 + 4\hat{y}^4) \hat{p}_1 \hat{P}_2 - 2\beta u \hat{X}_1 (\hat{y} + \hat{y}^2 + \hat{y}^3 + \hat{y}^4) \hat{X}_2 \\ &\quad + i\beta u (\hat{y} + 2\hat{y}^2 + 3\hat{y}^3) \hat{p}_1 + 4(\hat{y} + 2^2\hat{y}^2 + 3^2\hat{y}^3) \hat{p}_1^2 \hat{P}_2 - 4\beta u \hat{X}_1 (\hat{y} + 2\hat{y}^2 + 3\hat{y}^3) \hat{X}_2 \hat{p}_1. \end{aligned} \quad (3.13d)$$

At this point (having been convinced that the behavior described here is indeed valid for all orders of β), the summation is straightforward.

The results obtained so far are general. They may be used to describe the evolution of any signal or pump state in a DPA (although the choice of signal quadrature operators was specifically intended to simplify the study of squeezed-vacuum states).

The next step is calculating the matrix elements $\langle \hat{Q}_i \hat{Q}_j \rangle$. Working in the differential representation

$$\hat{Q}_1 = Q_1, \quad \hat{Q}_2 = -\frac{i}{2} \frac{\partial}{\partial Q_1}, \quad (3.14)$$

the quadrature operators are written as functions of \hat{X}_1 and \hat{P}_1 only, both of which are Hermitian:

$$\hat{Q}_1^n \hat{Q}_2^m \rightarrow \left(-\frac{i}{2}\right)^m Q_1^n \frac{\partial^m}{\partial Q_1^m}, \quad (3.15a)$$

$$\hat{P}_1^i \hat{P}_2^j \hat{X}_1^n \hat{X}_2^m \rightarrow \left(-\frac{i}{2}\right)^{j+m} P_1^i \frac{\partial^j}{\partial P_1^j} X_1^n \frac{\partial^m}{\partial X_1^m}. \quad (3.15b)$$

By writing the dominant term result in the $X_1 P_1$ representation, the matrix element reduces to a simple c -number, integral form

$$\begin{aligned} \langle \Psi | \hat{Q}_i \hat{Q}_j | \Psi \rangle &= \langle \Psi | \hat{Q}_i^\dagger \hat{Q}_j | \Psi \rangle \\ &= \int_{-\infty}^{\infty} dX_1 dP_1 \langle \Psi | \hat{Q}_i^\dagger | X_1 P_1 \rangle \langle X_1 P_1 | \hat{Q}_j | \Psi \rangle \\ &= \int_{-\infty}^{\infty} dX_1 dP_1 [\hat{Q}_i \Psi^*(X_1, P_1)] [\hat{Q}_j \Psi(X_1, P_1)], \end{aligned} \quad (3.16)$$

which may then be calculated either symbolically or numerically [depending on the wave function $\Psi(X_1, P_1)$].

The application of the dominant term method, as described in this section, was motivated by the work of CB. It was shown that the dynamics of the time-evolved quadrature operators of the DPA can be well approximated by an expression consisting of a few compact terms [up to $O(1/\alpha^4)$]. The results are comparable to sophisticated numerical methods (see Sec. VI).

The success of the dominant term method of this section is conditional upon the convergence of the sums obtained. At the same time, the faster these series converge, the less significant their summation to all orders. We have found that the recurring factor in all the series (dominant and next-to-dominant terms alike) was $\hat{y} \propto e^{2u}/\alpha^2$, which is negligible for typical systems, but could still offer some new insight for small α .

We are therefore led to conclude that the long-time behavior of the system ($u \gg u_{\text{min}}$, where u_{min} is the optimal interaction time) is primarily determined by "less dominant" terms. It is not known whether these terms can be written in series form and if so, whether these series converge, but any attempt to answer these questions would surely involve long, cumbersome calculations and would most likely be unrewarding. Thus the question of the behavior of the system at longer times remains, for the time being, an open one.

IV. METHOD OF PADÉ APPROXIMANTS

An alternative approach to the problem is trying to improve the convergence of truncated series without adding or removing any terms to the order of the truncation. Power series expansions converge only up to the pole

nearest the origin in the complex plane. Thus polynomial expansions of a function to finite order cannot give the behavior beyond the first pole. By contrast, other expansion schemes are not limited to a radius of convergence determined solely by the pole structure of the function.

One such expansion scheme is the method of Padé approximants [17,18], which we use here. This method seeks to increase the regime of convergence by "simulating" the real pole structure of the function. This is done by replacing a (divergent) power series representation $S(z)$ of some physical function $f(z)$ by a Padé approximant $P_M^N(z)$: a sequence of rational functions (or ratio of polynomials), which is then recast into a continued fraction form $F_N(z)$:

$$P_M^N(z) = \frac{\sum_{n=0}^N A_n z^n}{\sum_{n=0}^M B_n z^n}$$

$$\Rightarrow F_N(z) = \frac{1}{1 + \frac{C_1 z}{1 + \frac{C_2 z}{1 + \dots + \frac{C_{n-1} z}{1 + C_n z}}}} \quad (4.1)$$

The coefficients C_n (or A_n and B_n) are chosen so that the Taylor series expansion of the Padé approximant matches the first terms of the power series. For Padé approximants to converge, $F_N(z) \rightarrow f(z)$ [or $P_M^N(z) \rightarrow f(z)$] as N (or N, M) $\rightarrow \infty$, and $f(z)$ must be analytically continuable.

In our problem, $f(z)$ represents the matrix elements of the time-evolved quadrature operators, as given by the expansion to all orders of β . The power series representation $S(z)$ is the corresponding truncated series result, which in our case includes all terms to $O(\beta^4)$. Clearly, by neglecting higher-order terms, one would expect this limited power series representation of the solution to diverge after some time. Therefore, by rewriting the power series $S(z)$ in the form of Padé approximants, it may be possible to increase the region of convergence, thus achieving a better approximation (valid for longer times) to the full, exact solution. As the number of terms in the new expression grows, so does its region of convergence [19].

V. ENERGY CONSERVATION, UNITARITY, AND COMMUTATORS

In this section, we present two ways to check our results. One test—the commutator test—is applied only to the dominant term results. The second test directly measures energy conservation and can, in principle, be applied to any of our results. Both the commutator and the energy tests require all the quadrature operators to be calculated.

How important are the terms less dominant in u that the dominant term method neglects? We tackle this question by testing the commutation relations between the time-evolved quadrature operators. This test is used both to verify the validity of our results over the time-domains of primary interest to us and to find out when the dominant term method breaks down.

The quantum mechanical evolution of states is by definition unitary. Expressions describing nonunitary evolution point to a divergence from this physical condition. For well behaved states (that conserve energy), the commutation relations [Eqs. (3.12)] will hold as long as unitarity is preserved. Thus we use this test to indirectly check the unitarity of the time-evolved operators, as described by our approximations.

The expectation that unitarity fail at some point and hence that the commutation relations will not be obeyed applies only to the dominant term summations. For every order of perturbation of the equations of motion, unitarity is preserved. Accordingly, the truncated results pass the commutator test for all times. Further, the analytic continuation of these results, in the form of Padé approximants, does not in any way violate the commutation relations. Similarly, the power series summation according to the dominant term method over all orders of β preserves unitarity. The violation originates only when we discard less dominant terms within each order of β .

Hence, in the dominant term results, as long as the summed contribution of the neglected, relatively insignificant terms remains small, the divergence from the commutation relation will barely be noticeable; as time advances, the weight of these terms grows and their overall sum becomes increasingly important. The commutator test allows us to find the time u_{\max} after which the dominant term method ceases to be valid.

Using the fact that states with real wave functions obey

$$\langle \Psi | \hat{Q}_1 \hat{Q}_2 | \Psi \rangle = \int_{-\infty}^{\infty} dQ_1 Q_1 \Psi^*(Q_1) \left(-\frac{i}{2} \frac{\partial}{\partial Q_1} \right) \Psi(Q_1)$$

$$= -\langle \Psi | \hat{Q}_2 \hat{Q}_1 | \Psi \rangle, \quad (5.1)$$

Eqs. (3.12a) and (3.12b) may be rewritten, yielding

$$\langle [\hat{Q}_1, \hat{Q}_2] \rangle = 2\langle \hat{Q}_1 \hat{Q}_2 \rangle = \frac{i}{2}. \quad (5.2)$$

Thus the commutator test translates to calculating $\langle \hat{X}_i \hat{X}_j \rangle$, $\langle \hat{P}_i \hat{P}_j \rangle$, and $\langle \hat{X}_i \hat{P}_j \rangle$.

The approximations involved in obtaining the truncated results (and the Padé approximant results), namely, dropping all terms of $O(\beta^5)$ and higher, are very different from the dominant term method approximations. One implication we have seen is that the commutator test is meaningful only for the dominant term results. In what follows, we describe a simple, more generally applicable test, checking that the mean free energy of the fields $\langle \hat{\mathcal{H}}_0 \rangle$ [from Eq. (1.1)] is conserved [20]:

$$\hbar\omega_p \langle \hat{a}_p^\dagger \hat{a}_p \rangle + \hbar\omega \langle \hat{a}^\dagger \hat{a} \rangle = \text{const.} \quad (5.3)$$

Therefore, for an initial pump state $|\alpha = \sqrt{N}\rangle$ and a signal in vacuum,

$$2\bar{N}_p(u) + \bar{N}_s(u) = 2\bar{N}, \quad (5.4)$$

where

$$\bar{N}_p(u) = \langle \hat{P}_1^2 \rangle + \langle \hat{P}_2^2 \rangle - \frac{1}{2}, \quad (5.5a)$$

$$\bar{N}_s(u) = \langle \hat{X}_1^2 \rangle + \langle \hat{X}_2^2 \rangle - \frac{1}{2}. \quad (5.5b)$$

Since all our methods allow us to calculate any quadrature operator, Eq. (5.4) may be used as a test of their validity [21].

Let us look at Eq. (5.4) in a different light—not as a statement of energy conservation but as a measure of signal-pump entanglement [10,11]. To that end, we turn once again to the semiclassical approach.

Consider a time $u > u_{\min}$ when both signal quadratures are expected to grow exponentially:

$$\hat{X}_1(u) = \hat{X}_1(0)e^u, \quad (5.6a)$$

$$\hat{X}_1(u) = \hat{X}_2(u_{\min})e^{u-u_{\min}}. \quad (5.6b)$$

Using Eqs. (2.17), (2.16), and (5.5b), we obtain

$$\bar{N}_s = \left(1 + \frac{1}{16\bar{N}}\right) \langle \hat{X}_1^2 \rangle - \frac{1}{2}. \quad (5.7)$$

In this way, Eq. (5.4) reduces to a relation between the variances of \hat{X}_1 and \hat{P}_1 ,

$$\langle \hat{P}_1^2 \rangle = \frac{1}{4} + \bar{N} - \frac{1}{2} \left(1 + \frac{1}{16\bar{N}}\right) \langle \hat{X}_1^2 \rangle, \quad (5.8)$$

and in the limit of large \bar{N} ,

$$\langle \hat{P}_1^2 \rangle \simeq \bar{N} - \frac{1}{8}e^{2u}. \quad (5.9)$$

In this limit, assuming [21]

$$\langle (\hat{P}_2)^2 \rangle \lesssim \frac{1}{4}, \quad (5.10)$$

we see that the mean number of photons in the pump is approximately given by

$$\bar{N}_p \lesssim \bar{N} - \frac{1}{8}e^{2u} - \frac{1}{4}. \quad (5.11)$$

Hence, by imposing the energy-conservation condition on the semiclassical results, we are able to see the effect of pump depletion, at least phenomenologically.

Energy conservation and commutation relations are both consequences of unitarity. However, both these tests are indirect and incomplete tests of unitarity. Passing them is by no means a guarantee that the system described by our approximations evolves unitarily. Still, we will find (in the following sections) that such tests are informative and easy to perform. In addition, other calculations could be used as supplemental tests of our results. These include the calculation of other matrix elements such as $\langle \hat{Q}_i \rangle$ and $\langle \hat{H}_{\text{int}} \rangle$.

VI. RESULTS: COHERENT-PUMP DPA

This section opens with a discussion of two sets of the dominant term results (see the discussion in Sec. III) for the evolution of the squeezed quadrature: a partial set of data consisting of the most dominant terms in u and the full data, which also include next-to-dominant terms (Fig. 3). We continue with the truncated and Padé approximant results for this quadrature operator (Fig. 4). In addition, both figures show KFD's numerical data, with which a detailed comparison is made below.

Figure 3 shows the standard deviation of the squeezed quadrature $\Delta\hat{X}_2$ as a function of dimensionless time $u = \kappa\alpha t$, as calculated by the dominant term method. On the plot, the full dominant results are represented by a solid line, and the results for the dominant terms (excluding next-to-dominant terms) are plotted in dashed lines. Numerical data calculated by Kinsler *et al.* are plotted for comparison in dotted lines. The time at which optimal squeezing is obtained is denoted by u_{\min} (u_{\min}^{dom} for the full dominant results and later on u_{\min}^{trunc} , $u_{\min}^{\text{Padé}}$, and u_{\min}^{KFD} for the results of the truncated, Padé approximant, and numerical stochastic methods, respectively).

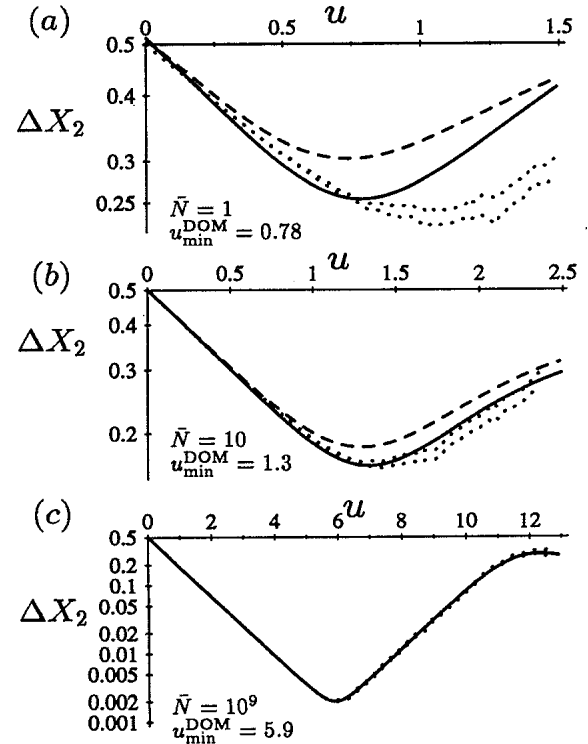


FIG. 3. Dominant term results for a coherent-pump DPA: ΔX_2 as a function of interaction time u for pump amplitudes of (a) $\bar{N} = \alpha^2 = 1$, (b) $\bar{N} = \alpha^2 = 10$, and (c) $\bar{N} = \alpha^2 = 10^9$. The dominant terms are drawn in dashed lines and the full dominant results (including next-to-dominant terms) are plotted in solid lines. For comparison, numerical stochastic data [8] are shown in the two dotted lines that correspond to one standard deviation up and down from the mean (not plotted). The optimal squeezing times of the full dominant results u_{\min}^{dom} are listed on the plots.

The three figures [3(a), 3(b), and 3(c)] show the results for $\bar{N} = 1, 10,$ and 10^9 on a log plot.

As expected, Fig. 3 shows increased squeezing up to some time u_{\min}^{dom} , followed by noise amplification. By the time a maximum is reached in $\Delta\hat{X}_2$ (for instance, $u \simeq 11.5$ for $\bar{N} = 10^9$), we expect pump depletion to take effect, leaving us with a weak pump and a noisy signal. It is difficult to tell how reliable the dominant term expansion scheme will be at such a time. We hope to determine when the dominant term method fails (whether after the noise is maximized or before) by the commutator test and by comparison with other data.

As an example of a strong pump field, we choose $\bar{N} = 10^9$ photons. The corresponding results [Fig. 3(c)] show a substantial reduction in the noise (almost 2.5 orders of magnitude, i.e., almost 50-dB reduction in the noise power), which agrees almost exactly with semiclassical predictions. For small photon numbers [$\bar{N} = 1$ and 10 in Figs. 3(a) and 3(b), respectively], the squeezing is of course much weaker. *A priori*, we may expect the results for very small photon numbers (or large expansion parameter β) to diverge because of the $(1/\alpha)$ expansion on which the dominant term scheme is based [22]. Hence the success of this method in qualitatively describing the

evolution beyond the time of optimal squeezing is itself encouraging.

In addition to the choice of expansion parameter, the dominant term method neglects terms with a weak time dependence. However, for the combination of very short times and very weak pumps, $u = \kappa\alpha t$ is small and no terms may be neglected. Thus we find that in Fig. 3(a), the dominant terms solution breaks down (i.e., $\Delta\hat{X}_2 \neq 1/2$) for $u \ll 1$. In fact, this minor flaw is a recurring one: for all the quadrature operators calculated (according to the dominant term method and the Padé approximant method), we find that the $\alpha = 1$ results for the $u \ll 1$ regime are wrong. The fact that this flaw appears only for very short times and very weak pumps in effect emphasizes the validity of our approximations for the interaction times and pump amplitudes that are of interest to us.

As the mean number of photons rises, one would expect the dominant term results to improve in accuracy and to yield reliable results for longer interaction times. Note, however, that for any fixed time u , as $\beta \rightarrow 0$, the importance of next-to-dominant terms diminishes. It is only as we move on to longer times (for which these terms include expressions like $e^{\alpha u}$) that these terms begin to dominate over the zeroth-order terms.

The calculations performed included three sets of results: the most dominant terms (dashed lines on Figs. 3, 5, and 6), the next-to-dominant terms (first correction terms, not plotted), and their sum (solid lines on the

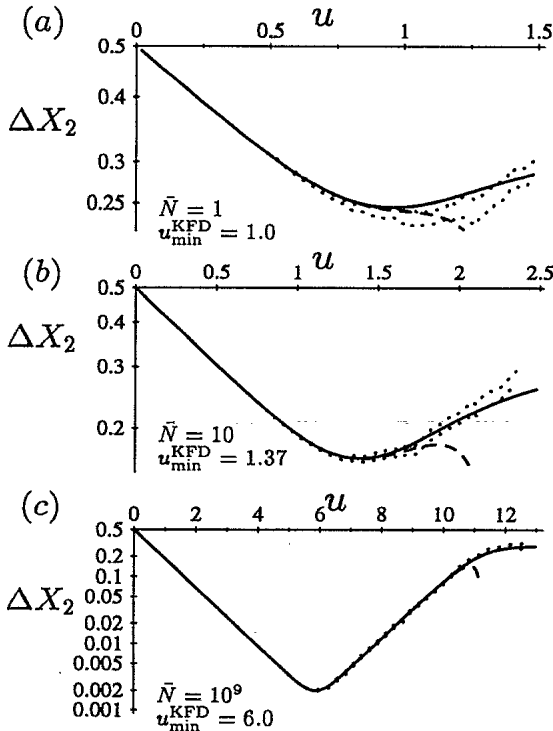


FIG. 4. Truncated and Padé approximant results for a coherent-pump DPA: ΔX_2 as a function of interaction time u for pump amplitudes of (a) $\bar{N} = \alpha^2 = 1$, (b) $\bar{N} = \alpha^2 = 10$, and (c) $\bar{N} = \alpha^2 = 10^9$. The truncated Padé results are drawn in dashed lines and the corresponding Padé approximant results are plotted in solid lines. Numerical stochastic data are drawn in dotted lines (as in Fig. 3). The optimal squeezing times of the numerical stochastic results u_{\min}^{KFD} , as calculated by Kinsler *et al.* [8], are listed on the plots. The optimal times as calculated by the truncated and Padé approximant methods are given in Figs. 7 and 8.

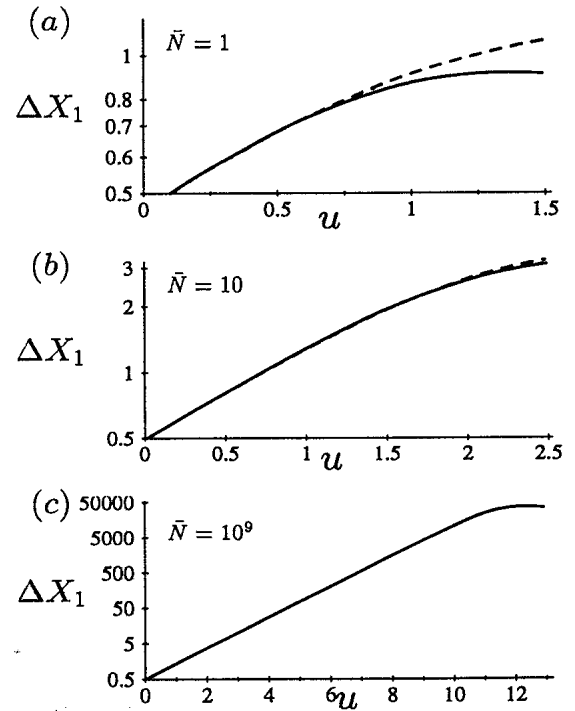


FIG. 5. Dominant term results for a coherent-pump DPA: ΔX_1 as a function of interaction time u for pump amplitudes of (a) $\bar{N} = \alpha^2 = 1$, (b) $\bar{N} = \alpha^2 = 10$, and (c) $\bar{N} = \alpha^2 = 10^9$. The dominant terms are drawn in dashed lines and the full dominant results (including next-to-dominant terms) are plotted in solid lines.

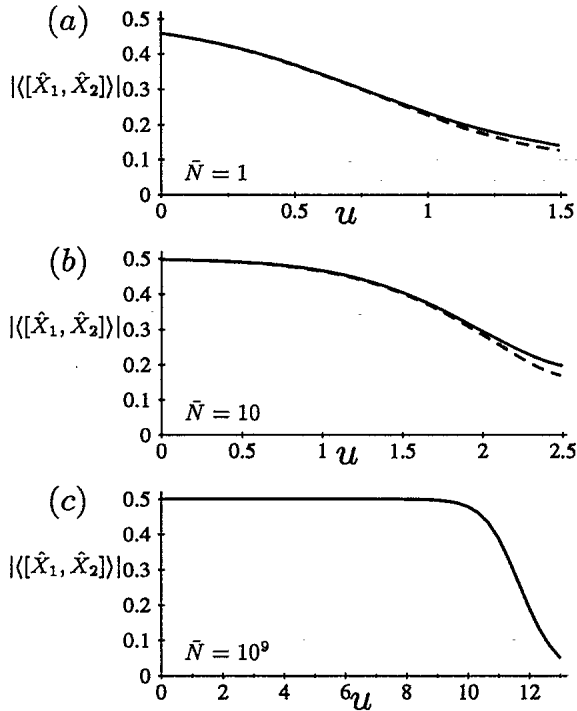


FIG. 6. Dominant term results for a coherent-pump DPA: $|\langle[X_1, X_2]\rangle|$ as a function of u for pump amplitudes of (a) $\bar{N} = \alpha^2 = 1$, (b) $\bar{N} = \alpha^2 = 10$, and (c) $\bar{N} = \alpha^2 = 10^9$. The dominant terms are drawn in dashed lines and the full dominant results (including next-to-dominant terms) are plotted in solid lines.

same graphs). In the case of $\bar{N} = 10^9$, the (most) dominant term results and the full dominant results appear indistinguishable when plotted on the same graph, and the next-to-dominant terms tend to zero. A closer look at the data for these full results confirms this: The next-to-dominant terms are smaller than the dominant terms by $O(\beta^2)$, as predicted, and hence are significant only for $\bar{N} \sim 1-10$. And indeed, the differences in these plots clearly point to the contribution of the next-to-dominant terms, even for very small times. These terms improve (i.e., lower) and delay the minimum noise. However, the size of the contribution serves to remind us that the next correction (consisting of many more terms) may be substantial for these times and pump intensities as well.

The importance (or lack thereof) of the next-to-dominant terms teaches us about the success of our model. If important, we may gain information about the long-time behavior of the DPA, which we could not derive from the dominant terms alone. This might also serve as an incentive to attempt to calculate less dominant terms in the hope that with each additional step we would describe the system for longer and longer times. On the other hand, with each step the task would become harder; summation of terms based on patterns of power series would be practically impossible. Conversely, if the next-to-dominant terms do not appear to improve the convergence of our results, we may infer either that the function is not convergent or that this method does not offer a feasible means to get converg-

ing results for times longer than may already be obtained from the dominant terms. The expansion parameter tells us that the importance of the next-to-dominant terms is inversely proportional to the pump strength: The weaker the pump, the larger the contribution from less dominant corrections. While this method may fail in the limit of a weak pump (when the expansion parameter is too large), for a very strong pump, the dominant terms alone may, with high likelihood, provide an accurate description of the squeezing. If true, the above result might in fact be encouraging and lead us to conclude that the dominant term summation method, when applied only to dominant terms (which are given by short and simple analytic expressions), yields comparatively good results.

Let us now see how the dominant term method results for $\Delta\hat{X}_2$ compare with the other methods we have used. The dashed lines on Fig. 4 represent the truncated result (see Sec. III). This method is a straightforward expansion in β and keeps all terms up to the order of the perturbation $O(\beta^4)$. As in the dominant term method, by the very nature of the expansion scheme, we cannot expect exceedingly accurate results for small mean photon numbers.

We begin with a brief comparison of the truncated series and dominant term data. For $\bar{N} = 1$ [Figs. 3(a) and 4(a)], these data agree only for very short time and the truncated results fail long before the optimal squeezing time. Already for $\bar{N} = 10$ [Fig. 4(b)], a minimum can clearly be seen, but the solution breaks down immediately after u_{\min}^{trunc} ; these data agree with the dominant term solution to within a few percent error until after u_{\min} . In Fig. 4(c) ($\bar{N} = 10^9$), we find a result very similar to the dominant term result, although it seems to break down slightly earlier (but still considerably after u_{\min}^{trunc}).

Applying the method of Padé approximants to these results yielded the graphs shown by the solid lines (Fig. 4). We see that in all three plots of this figure [(a)–(c)], the truncated results and the corresponding Padé approximant results are practically identical before the minima are reached and for all times until the truncated method begins to fail. (Thus for $\bar{N} = 10$ and 10^9 , we find that $u_{\min}^{\text{trunc}} = u_{\min}^{\text{Padé}}$ [23].) While for $\bar{N} = 1$ we find a discrepancy between the Padé approximant and dominant term results that grows as the minimum is passed, the curves for stronger pumps reveal better convergence. This is clearly manifested in the long-time results in the $\bar{N} = 10^9$ case, where we find that the variance asymptotically approaches a maximum; the Padé approximant and dominant term data are barely distinguishable.

The three sets of $\Delta\hat{X}_2$ results presented above [Figs. 3(c) and 4(c)] are in close agreement for $\bar{N} = 10^9$, but differ for very weak pumps. In the case of the dominant term results, we also found differences between the dominant term calculation and the full data (including next-to-dominant terms).

The validity of each and all the above results must be checked. Clearly the qualitative behavior meets our expectations. We would now like to quantitatively assess the results in order to try and answer the following questions: Do any of the methods provide long-time informa-

tion on the system's evolution, in particular for strong pumps? Can we confirm the numerical calculations in the literature? How useful are our methods for relatively weak pumps? Before answering these questions, we turn to the dominant term results for the conjugate, amplified quadrature.

Squeezing implies the reduction of noise in one quadrature at the expense of the conjugate quadrature. We have seen the effect of squeezing on the \hat{X}_2 quadrature. We now turn to the time development of the amplified quadrature. Semiclassical calculations predict pure squeezing until u_{\min} is reached. After that time, the uncertainties in both quadratures undergo amplification so that the signal state ceases to be a minimum uncertainty state. Our motivation is twofold: First, we would like to verify this "antisqueezing" effect on \hat{X}_1 , and second, the calculation of the conjugate quadrature's evolution is to be used in the commutator test.

The plots for these results (Fig. 5) include the most dominant terms (dashed line) and the full dominant result (solid line). We note that the role of the next-to-dominant terms for small photon numbers sets in only at long times (approximately at u_{\min}^{dom} for $\bar{N} = 1$ and even later for $\bar{N} = 10$). The increase in the noise for this quadrature is exponential at first, as predicted semiclassically. Since the mean photon number in the signal is

$$\bar{N}_s \propto \langle \hat{X}_1^2 \rangle = \Delta \hat{X}_1^2, \quad (6.1)$$

one would expect the amplification to cease when the signal has reached an intensity of $O(\bar{N})$. The $\langle \hat{X}_1^2 \rangle$ data for these times according to the dominant term method are

$$\begin{aligned} \langle (\hat{X}_1^{\max})^2 \rangle &= 0.82, & 2\bar{N} &= 2; \\ \langle (\hat{X}_1^{\max})^2 \rangle &= 9.78, & 2\bar{N} &= 20; \\ \langle (\hat{X}_1^{\max})^2 \rangle &= 1.28 \times 10^9, & 2\bar{N} &= 2 \times 10^9. \end{aligned} \quad (6.2)$$

These results also indicate that when this stage is reached, the pump is already depleted.

There are many possible ways to analytically check the validity of our results. Here we use one test—the commutator test—to check results obtained via the dominant term method. In addition, we suggest a second test to directly measure energy conservation. This latter test (the energy test) can, in principle, be applied to any of our results.

For the commutator test, we concentrate on the calculations of the mean commutator of the signal quadrature operators $\langle [\hat{X}_1, \hat{X}_2] \rangle$ in the dominant term method. For states with real wave functions (including any state that has a reflection symmetry in phase space),

$$\langle [\hat{Q}_1, \hat{Q}_2] \rangle = 2\langle \hat{Q}_1 \hat{Q}_2 \rangle = \frac{i}{2} \quad (6.3)$$

(see Sec. V). As long as Eq. (6.3) is obeyed by both signal and pump, we expect that the dominant term expansion scheme is good. The pump commutator test showed that the pump commutator remains constant for longer times [24]. It remains for the signal commutator test to deter-

mine the reliability range of the dominant term method. At this point, we do not rule out the possibility that evolution described by the dominant term method may be relatively accurate even for longer times. However, beyond the range of the commutator-preserving results, we must also check our results by comparing them to data obtained by other, independent methods.

The results—plots of $|\langle [\hat{X}_1, \hat{X}_2] \rangle|$ as a function of u —are shown in Fig. 6. In the case of $\bar{N} = 1$, the commutator test fails for all times. Equation (6.3) is not obeyed even at $u = 0$. A slight improvement can be found in Fig. 6(b) for $\bar{N} = 10$. This result, as mentioned before, was not unexpected for these values of β , especially after seeing the plot of the dominant term results deviate from the truncated and Padé approximant data [25]. As the pump strengthens, the dominant term and Padé approximant results agree for longer times, and the corresponding commutator results [Fig. 6(c)] improve as well [26]. Optimal squeezing for a pump of $\bar{N} = 10^9$ was found to be at $u_{\min} \ll u_{\max}$ and may therefore be considered valid on all grounds: a comparison with truncated and Padé approximant results and the outcome of the commutator test. However, the commutation relations fail before any discrepancy can be discerned between the dominant term and Padé approximant data. Could this imply that all of these results are flawed for $u > u_{\max}$? We deem this possibility unlikely but prefer not to disregard it altogether.

Had we not tested the commutation relations of the system's evolution, we might rely on the results in Fig. 3(b) until $u \sim 1.6$ and on those of Fig. 3(c) until $u \sim 11$ or longer. After all, the behavior appears reasonable for those times. Apparently, the commutator calculation is a more sensitive test of the results. Although it may prove too strict for our purposes, we find it useful and reassuring in the case of a strong pump.

We have presented the results for the evolution of the squeezed signal quadrature of the DPA with a coherent pump according to three methods: summation of dominant and next-to-dominant terms, truncated series, and a Padé approximant representation of the truncated series. The dominant terms in u have been calculated by a scheme similar to our dominant term method prior to this work, but were not summed to all orders of β [7]. These results are very similar to the (most) dominant term result (dashed line in Fig. 3). The truncated results for $\Delta \hat{X}_2(u)$ have also been calculated by CB to $O(\beta^4)$. We now compare our findings with KFD's results [8], shown in dotted lines on Figs. 3 and 4. The two lines represent upper and lower standard deviation marks for the data. (The error arises from the details of the stochastic calculation that was employed.)

In the $\bar{N} = 1$ case, the curve obtained from the (full) dominant term data differs most from KFD's, while the truncated result diverges around $u \simeq 0.7$. In spite of its divergence from the numerical results, the dominant term method gives a better qualitative description of the evolution than the truncated and Padé approximant methods for longer times. The Padé approximant results lie outside the first standard deviation range of KFD's data for some time after the minimum, but not by far and only for a relatively short time.

For $\bar{N} = 10$, we note the improvement in all the results and in particular in the dominant term method results. We find that the full dominant results agree with KFD's data for most of the time and diverge from them only by 1–2%. This convergence of the results continues for as long as the KFD data are available. The Padé approximant results are similar, fitting well with KFD's data and slightly diverging from them at very long time ($u \gtrsim 2.2$). The location of the minimum u_{\min}^{KFD} is given by all of the methods to within 2%. By this time, there is no doubt that the truncated series data lag behind the other methods. This only emphasizes the problematic nature of straightforward, unaided perturbation theory. We see that either by adding more (correctly chosen) terms to the final expressions (the dominant term scheme) or by rewriting the matrix elements (the method of Padé approximants), we are able to considerably improve our solutions and our data compare favorably to KFD's numerical solutions.

This conclusion is supported by the $\bar{N} = 10^9$ data as well. For a sufficiently strong pump, we find that data obtained from the dominant term method, from the Padé approximants method, and from KFD's stochastic methods agree almost perfectly for all time; in contrast, the truncated results improve as the pump intensifies but do not provide long-time information on the system. The optimal squeezing time is given to within 1.7% by the four methods. Finally, we consider the importance of the commutator test for this case—the sole case that validated dominant term results at least for $u \lesssim u_{\max}$. Since we have no definite explanation of the declining commutator results and wish to test our methods even (or especially) when results are not available from the literature, we choose to be conservative and adopt the commutator test as a reliable measure of the convergence of the dominant term solutions and as a sensitive warning indicator. Having said that, we keep in mind that the results are likely to be valid for much longer times than guaranteed by the commutator test. Therefore, the one set of data (of the dominant method) we may fully trust is the $\bar{N} = 10^9$ data, for which, as we have seen, the next-to-dominant corrections are negligible. It is therefore sufficient to calculate the dominant terms, thereby obtaining simple analytic forms that compare with the Padé approximant results and KFD's data for all time, even when the pump is depleted.

Let us regard the calculations presented so far for the DPA with a coherent pump as an introduction and a preparation for what has yet to come. The goal of these calculations was to find viable techniques for the quantum mechanical study of light propagation in nonlinear media. We found that the method of Padé approximants offers good qualitative and reasonably good quantitative results in the limit of a weak pump ($\bar{N} \simeq 1$ to 10), while the results for stronger pumps are excellent by any available standard to date. Further, we found that the results of the dominant term and Padé approximant methods are in close agreement for intermediate and strong pumps ($\bar{N} \simeq 10$ – 10^9) and that the commutator test places an upper bound on the validity of the dominant term method. These conclusions give us confidence in

seeking solutions to the signal evolution for an arbitrary pump state. We now turn to a discussion of squeezing in a DPA with a quadrature-squeezed pump.

VII. RESULTS: SQUEEZED-PUMP DPA

We now describe the results for the noise reduction in a DPA with a squeezed pump obtained by the method of truncation, Padé approximants, and summation over dominant terms. The truncated and Padé approximant results are given for pump intensities of $\alpha^2 = 1$, 10, and 10^9 (Figs. 7 and 8, respectively). The full dominant results are given for $\alpha^2 = 10^9$ (Fig. 9) since only for this pump intensity were we able to verify the corresponding coherent-pump results by the commutator test.

Semiclassically, except for a slight increase in the timing and extent of the optimal squeezing [Eq. (2.26)], this system's behavior is the same as that of a DPA with a coherent pump. Our results show this shift in the position of the minimum variance with the growing squeezing parameter of the pump r . In addition, we see the amplifying effect of a negatively squeezed (i.e., number-squeezed) pump on the signal noise, for the case of $\alpha^2 = 1$ [Figs. 7(a) and 8(a)]. These results confirm our prediction regarding the shift in the location of the optimal signal squeezing [$\langle(\Delta\hat{X}_2)_{\min}^2\rangle$ and u_{\min}] due to pump squeez-

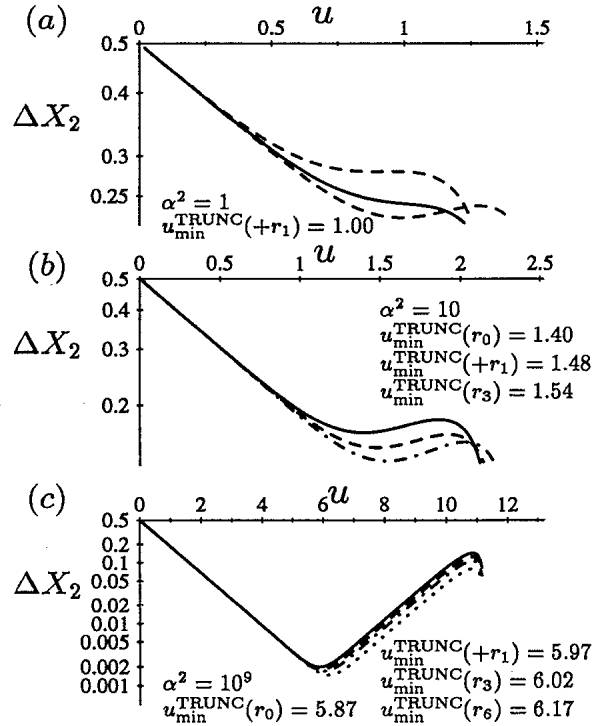


FIG. 7. Truncated results for a squeezed-pump DPA: ΔX_2 as a function of u for pump amplitudes of (a) $\alpha^2 = 1$, (b) $\alpha^2 = 10$, and (c) $\alpha^2 = 10^9$. The calculations were performed for a coherent pump ($r = r_0 = 0$, solid lines) and for the following pump squeezing parameters: $r_1 = \pm 0.15$ (dashed lines), $r_3 = 0.3$ (dash-dotted lines), and $r_6 = 0.6$ (dotted lines). The optimal squeezing times of the truncated results $u_{\min}^{\text{TRUNC}}(r)$ are listed on the plots.

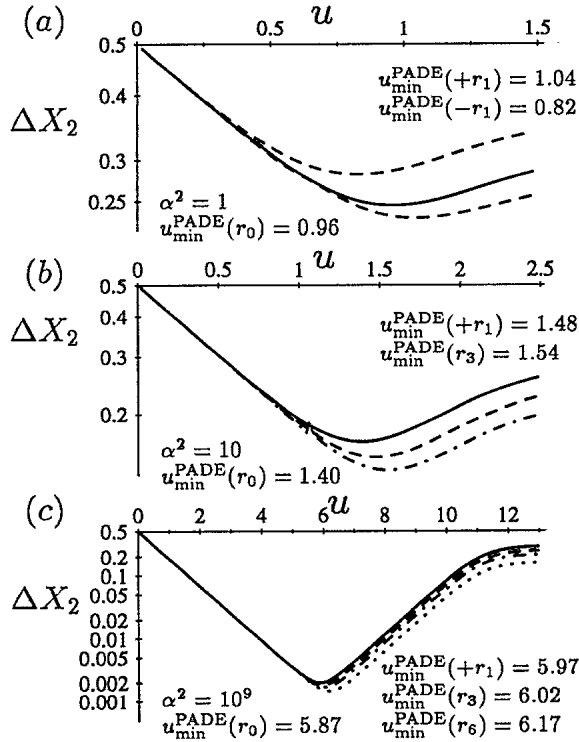


FIG. 8. Padé approximant results for a squeezed-pump DPA: ΔX_2 as a function of u for pump amplitudes of (a) $\alpha^2 = 1$, (b) $\alpha^2 = 10$, and (c) $\alpha^2 = 10^9$. The calculations were performed for a coherent pump ($r = r_0 = 0$, solid lines) and for the following pump squeezing parameters: $r_1 = \pm 0.15$ (dashed lines), $r_3 = 0.3$ (dash-dotted lines), and $r_6 = 0.6$ (dotted lines). The optimal squeezing times of the Padé approximant results $u_{\min}^{\text{Padé}}(r)$ are listed on the plots.

ing. While pump squeezing has no effect on the signal for interaction times of $u < u_{\min}$ (coherent pump), we find that a slightly longer interaction time would improve the squeezing. The larger the pump squeezing r , the longer the time needed to obtain the optimal \hat{X}_2 variance (as noted on these figures). These results are confirmed by the (full) dominant term data [Fig. 9(b)], where the squeezing parameters used are $r = 0, -0.1$, and 0.6 .

The fact that for a weak pump we find that there exists an optimal squeezing parameter, above which the signal squeezing begins to deteriorate (as seen by Hillery *et al.* [9]), may seem surprising at first. This is a direct result of pump intensity fluctuations as was obtained semiclassically in Sec. II. We propose that this effect is caused by the large pump uncertainty along the \hat{P}_1 quadrature (Fig. 10). The quadrature-squeezed pump is represented by an ellipse in phase space (with $\Delta\hat{P}_1$ and $\Delta\hat{P}_2$ as major and minor axes, respectively). For large enough r and small enough α ,

$$\hat{P}_1 = \langle \hat{P}_1 \rangle + \Delta\hat{P}_1 \sim \alpha + \frac{e^r}{2} \simeq \frac{e^r}{2}. \quad (7.1)$$

This implies that some noise “spills over” to the opposite phase. In other words, some of the signal is squeezed along the conjugate quadrature while most of the signal noise is still squeezed in phase with the pump’s coherent amplitude. Thus we may sum over the contributions of

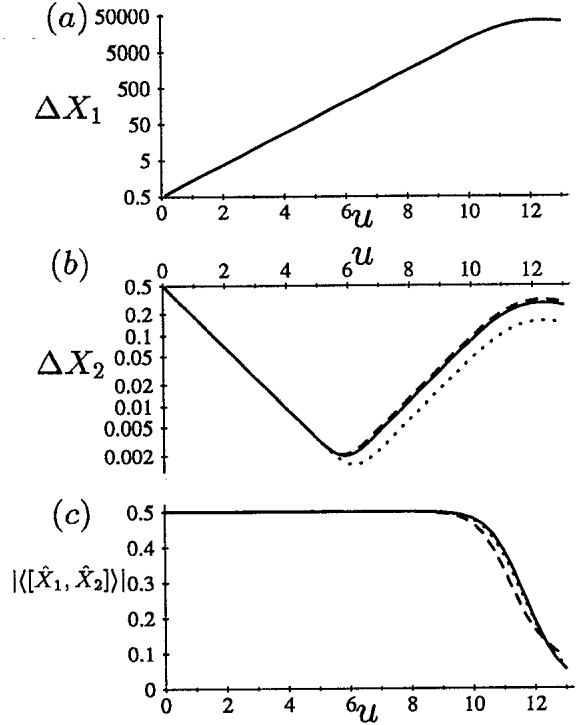


FIG. 9. Full dominant results for a squeezed-pump DPA with $\alpha^2 = 10^9$: The plots show (a) ΔX_1 , (b) ΔX_2 , and (c) $|\langle [\hat{X}_1, \hat{X}_2] \rangle|$ as a function of time u . The calculations were repeated for a coherent pump DPA ($r = 0$) and for the following pump squeezing parameters: $r = -0.1$ (dashed lines) and 0.6 (dotted lines). The optimal squeezing times of the full dominant results $u_{\min}^{\text{dem}}(r)$ are listed on the plots.

these two competing processes and see that they lead to a noisy signal.

As a numerical example, let us take $\alpha = 1$ and $r = 0.6$. Then, from Eq. (3.4),

$$\alpha + \langle \hat{P}_1 \rangle \sim \alpha = 1, \quad \Delta\hat{P}_1 \sim \frac{e^r}{2} = 1. \quad (7.2)$$

Here, the major axis of the ellipse represents a Gaussian noise profile with a width of $2\Delta\hat{P}_1 = 2$. Thus approximately 85% of the pump will squeeze the signal noise along the X_2 quadrature while the remaining 15% will amplify the signal noise along that quadrature. In accor-

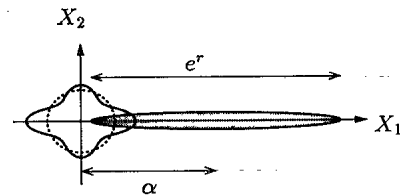


FIG. 10. DPA with a weak, squeezed pump: A pump (drawn in gray) with a squeezing parameter r and a real coherent amplitude α interacts with a signal in vacuum (dotted circle) and squeezes it along both the X_1 and the X_2 quadratures (solid line). Squeezing along the X_1 quadrature is a direct result of the pump noise “spilling over” to negative phases, such that the mean signal phase becomes $\pm\pi/2$.

dance with the semiclassical model [27],

$$\langle \Delta \hat{X}_2^2 \rangle = 0.85 \left(\frac{e^{-2u}}{4} + \frac{e^{2u-2r}}{64\alpha^2} \right) + 0.15 \left(\frac{e^{2u}}{4} \right). \quad (7.3)$$

Minimizing the variance over time yields an optimal squeezing time of

$$u_{\min} = \frac{1}{4} \ln \left(\frac{0.85}{0.15 + 0.85 \frac{e^{-2r}}{16\alpha^2}} \right) = 0.41, \quad (7.4)$$

as opposed to our original semiclassical predictions of

$$u_{\min}(\alpha = 1, r = 0.6) = 1.0, \quad (7.5)$$

$$u_{\min}(\alpha = 1, r = 0) = 0.7. \quad (7.6)$$

These results can be taken yet another step if the effect of pump depletion is included as well. Then, as the pump weakens, more of its noise spills over to the opposite phase. However, rather than dwelling on more semiclassical corrections at this point, we now return to our discussion of the quantum mechanical solutions and their validity.

Once again, we use the commutation relations to test our dominant term results for the time-evolved squeezing in a squeezed-pump DPA. To that end, we have calculated the time-evolved amplified quadrature and used it to obtain the signal commutator $[\hat{X}_1(r, u), \hat{X}_2(r, u)]$. The expectation values are plotted in Figs. 9(a) ($\Delta \hat{X}_1$) and 9(c) (commutator) [28].

Unlike the squeezed-quadrature results, Fig. 9(a) shows that pump squeezing has no effect on $\Delta \hat{X}_1(u)$ (for a pump of $\alpha^2 = 10^9$) [29]. Interestingly, the pump squeezing parameter r does not appear in the expression for the most dominant terms. Since the next-to-dominant terms are negligible for this quadrature and this pump strength, we are not surprised to find that the amplified quadrature remains unaffected by pump squeezing. By examining Figs. 9(a) and 9(b), one sees that the signal continues to be in a minimum uncertainty state until $u_{\min}(r)$.

From the commutator test results, we find that the squeezing parameter has a small but noticeable effect. This effect comes in only via the next-to-dominant terms (since the dominant terms, like those of $\langle \hat{X}_1^2 \rangle$, have no r dependence). For all three values of r tested, commutation relations are preserved longer than u_{\min} , but are violated shortly afterwards. We find that the (full) dominant term results are valid for a slightly longer time when the pump is squeezed. Though in itself of dubious importance, this may be of use since the method of Padé approximants appears sensitive to very high squeezing parameters. Therefore, when interested in the dynamics generated by a DPA with an intense and highly squeezed pump, dominant term results may be the most reliable.

The literature on the dynamics of the DPA with arbitrary signal and pump states is very limited. The parametric oscillator (a relative of the parametric amplifier)

with a squeezed pump has been studied by Munro and Reid [30]. They found that the squeezing of the signal is improved if the pump is squeezed. Hillery *et al.* [9] approach the question of a DPA with a squeezed pump semiclassically. They find that in the case of a relatively weak pump (for instance, $\alpha^2 = 5$) and high enough pump squeezing ($r \simeq 2$), then within the time that the semiclassical assumptions hold, not only is signal squeezing not improved, but it in fact gets worse. This agrees with our semiclassical explanations in Sec. VII.

According to our semiclassical calculations, the pump noise fluctuations cause the signal noise to evolve according to two competing processes. The first and obvious process is signal squeezing in phase with the pump's coherent amplitude. In the case of a phase-squeezed pump, this results in signal squeezing beyond $u_{\min}(\text{coherent pump})$. The second effect—pump noise spillover onto negative phases—causes a deterioration in the signal squeezing. For typical pumps ($\alpha^2 \gtrsim 10$) and a reasonable amount of pump squeezing ($r \lesssim 1$), this latter effect is negligible. However, for pumps that are both sufficiently weak and sufficiently squeezed, these effects may both be observed. In particular, we have found that the noise-spillover effect dominates for very short times while the improvement in the signal squeezing due to reduced pump phase fluctuations becomes significant only after $u_{\min}(\text{coherent pump})$.

VIII. CONCLUSION

We conclude that the analytic techniques employed (namely, the dominant term expansion and summation scheme and the method of Padé approximants) lead to results that outdo other methods (path integrals [6] and numerical stochastic methods [8]) in both their simplicity and flexibility. Using these methods, we obtain not only the time-evolved squeezed quadrature but a much more complete picture of the dynamics of the system, which allows us to study the signal and the pump for arbitrary initial conditions as well as quadrature correlations and commutators.

In the case of a squeezed-pump DPA, we found when signal squeezing can be further improved by pump squeezing and explained our results using the phase space representation and by applying semiclassical considerations. In the limit of a weak pump, our results agree with the literature [9–11] as they do for a coherent pump [6–8].

ACKNOWLEDGMENTS

N.C. was funded by the Labov Memorial Fellowship and S.L.B. by a Feinberg Fellowship. The authors thank P. Kinsler for access to his numerical data, and N.C. thanks M. Hillery for discussions.

- [1] H. Takahashi, *Adv. Commun. Syst.* **1**, 227 (1965).
- [2] N. Bloembergen, *Nonlinear Optics* (Benjamin, New York, 1965).
- [3] W. H. Louisell, A. Yariv, and A. E. Siegman, *Phys. Rev.* **124**, 1646 (1961).
- [4] For the first demonstration of squeezing in a parametric oscillator (closely related to the parametric amplifier), see L.-A. Wu, H. J. Kimble, J. L. Hall, and H. Wu, *Phys. Rev. Lett.* **57**, 2520 (1986).
- [5] Squeezing with a 3.0-dB improvement over the shot-noise limit was achieved by M. Xiao, L.-A. Wu, and H. J. Kimble, *Phys. Rev. Lett.* **59**, 278 (1987).
- [6] M. Hillery and M. S. Zubairy, *Phys. Rev. A* **29**, 1275 (1984), and references therein.
- [7] D. D. Crouch and S. L. Braunstein, *Phys. Rev. A* **38**, 4969 (1988).
- [8] P. Kinsler, M. Fernée, and P. D. Drummond, *Phys. Rev. A* **48**, 3310 (1993).
- [9] M. Hillery, D. Yu, and J. Bergou, *Phys. Rev. A* **49**, 1288 (1994).
- [10] V. Bužek and G. Drobný, *Phys. Rev. A* **47**, 1237 (1993).
- [11] G. Drobný and V. Bužek, *Phys. Rev. A* **50**, 3492 (1994).
- [12] The term "small" is used here as a measure relative to the contribution of pump phase fluctuations [see C. M. Caves and D. D. Crouch, *J. Opt. Soc. Am. B* **4**, 10 (1987)].
- [13] We can arrive at the same approximation from simple trigonometric considerations: For large α , the first-order correction term is related to $\langle(\Delta\hat{X}_1^{(0)})^2\rangle$ by $\langle(\Delta\hat{X}_2^{(1)}(u))^2\rangle \simeq \langle[\Delta\hat{X}_1^{(0)}(u)]^2\rangle \langle\Delta\phi^2(u)\rangle$, yielding Eq. (2.15).
- [14] These operators, so defined, can be measured directly in the laboratory by a homodyne detection scheme. See H. P. Yuen, *Phys. Rev. A* **13**, 2226 (1976); for a review of homodyne detection see H. P. Yuen and J. H. Shapiro, *IEEE Trans. Inf. Theory* **26**, 78 (1980).
- [15] S. L. Braunstein and R. I. McLachlan, *Phys. Rev. A* **35**, 1659 (1987).
- [16] For a detailed description of this procedure, see [7]. Note that in their calculation, the term "dominant" refers to the exponential power alone, and all terms proportional to e^{Ju} are kept.
- [17] C. M. Bender and S. A. Orszag, *Advanced Mathematical Methods for Scientists and Engineers* (McGraw-Hill, New York, 1978), p. 383.
- [18] C. A. Baker, *Essentials of Padé Approximants* (Academic, New York, 1975).
- [19] It turns out that despite the smallness of N (and M), there can still be a substantial improvement in the convergence of the solution.
- [20] This is a consequence of the rotating-wave approximation in this Hamiltonian. This energy is also the total mean free energy of the system, because in our Hamiltonian $\hat{\mathcal{H}}_{\text{int}} = \text{const}$, and for the signal in vacuum $\langle\hat{\mathcal{H}}_{\text{int}}\rangle = 0$.
- [21] In fact, by choosing $\langle\phi\rangle = \langle\hat{P}_2\rangle = 0$ and $\langle\hat{P}_2^2\rangle = 1/4$, it is sufficient to calculate three quadrature operators. From our calculations, it appears that the approximation $\langle\hat{P}_2^2\rangle \simeq 1/4$ is valid for much longer times than are required for the energy test.
- [22] Note that as a consequence of our choice of expansion parameter, the methods presented in this paper may not be used to study a DPA with a pump with a zero coherent amplitude.
- [23] The optimal squeezing times on the plots refer to numerically obtained results. The optimal times according to the truncated series and Padé approximant calculations $u_{\text{min}}^{\text{trunc}}$ and $u_{\text{min}}^{\text{Padé}}$ are noted on Figs. 7 and 8, respectively.
- [24] For instance, in the case of $\bar{N} = 10^9$, we find that $u_{\text{max}} = 8.8$ for the signal and 9.2 for the pump.
- [25] Perhaps surprisingly, even though the dominant term data (dashed line) differ from the full dominant results (solid line) in Figs. 3(a) and 3(b) ($\Delta\hat{X}_2$ graphs), the commutator test fails equally in both.
- [26] We now find that until u_{max} , the commutator is exactly $i/2$ (up to numerical error).
- [27] This calculation sums the contributions at the probability level and not at the amplitude level.
- [28] The solid-line plots in Figs. 10(a), 10(b), and 10(c) are identical to the full dominant results in Figs. 3(c), 5(c), and 6(c). The scaling and normalization are also identical.
- [29] This justifies the semiclassical assumption in Sec. II that the corrections to $\Delta\hat{X}_1(u)$ due to pump squeezing are of no consequence to the first-order corrections $\Delta\hat{X}_2^{(1)}(u)$. Furthermore, the data show that effects such as pump depletion are not affected by pump squeezing.
- [30] W. J. Munro and M. D. Reid, *Quantum Opt.* **4**, 181 (1992).